Understanding the reversible anodic behaviour and fluorescence properties of fluorenylazomethines — A structure–property study

Satyananda Barik, Sayuri Friedland, and W.G. Skene

Abstract: A series of fluorenylazomethine dyads and triads were prepared by simple condensation between the corresponding amine and aldehyde fluorene derivatives. These compounds were prepared as model compounds for investigating the effects of substitution and electronic groups on both the electrochemical properties and fluorescence quantum yields. It was found that the oxidation potential could be decreased by both incorporating electron donating groups and increasing the degree of conjugation. It was further found that alkylation in the fluorene's 9-position increased the azomethine degree of conjugation by forcing all the fluorene moieties to be coplanar with the azomethine bonds to which they are attached. Meanwhile, reversible radical cation behaviour was possible by substituting the terminal 2,2′-positions with atoms other than hydrogen. The radical cation was theoretically found to be distributed evenly across the fluorene, corroborating the reversible anodic behaviour with 2,2′-substitution. The fluorescence quantum yields of the azomethines were not found to be dependent on substitution. This was because the azomethine fluorescence was found to be quenched relative to their precursors regardless of substitution. The fluorescence could be restored at both low temperature and by acid protonation.

Key words: fluorenylimines, reversible oxidation, cyclic voltammetry, azomethines, Schiff base, radical ions.

Résumé : On a préparé une série de dyades et de triades de la fluorénylazométhine par simple condensation entre des dérivés de l'amine et de l'aldéhyde du fluorène. On a préparé ces composés comme modèles pour des études sur les effets de substitution et des groupes électroniques tant sur les propriétés électrochimiques que sur les rendements quantiques de fluorescence. On a trouvé que le potentiel d'oxydation peut être réduit tant par l'incorporation de groupes électrodonneurs que par une augmentation du degré de conjugaison. On a aussi trouvé que l'alkylation en position 9 des fluorènes augmente le degré de conjugaison des azométhines en forçant toutes les entités fluorènes à être coplanaires avec les liaisons azométhines auxquelles sont attachées. Par ailleurs, un comportement de cation radical réversible est possible si l'on substitue les positions terminales en 2,2′ par des atomes autres que l'hydrogène. On a trouvé sur une base théorique que le cation radical peut être distribué d'une façon uniforme sur l'ensemble de la portion fluorène, ce qui confirme le comportement anodique réversible avec une substitution 2,2′. Les résultats obtenus suggèrent que les rendements quantiques de fluorescence des azométhines ne dépendent pas de la substitution. Cette conclusion repose sur le fait que la fluorescence de l'azométhine est désactivée par rapport à celles de leurs précurseurs quelle que soit la substitution. La fluorescence peut être restaurée aussi bien par une basse température que par une protonation acide.

Mots-clés : fluorénylimines, oxydation réversible, voltampérométrie cyclique, azométhines, base de Schiff, ions radicaux.

Introduction

Conjugated polymers are of great interest in part due to their electrochemical and optoelectronic properties that are well-suited for use in plastic devices such as organic field effect transistors (OFET), light emitting diodes (OLED), and organic photovoltaics (OPVD), to name but a few.[1–4] Polyfluorenes are particularly interesting because of their inherent fluorescence making them appropriate emitting materials for OLED usage.[5] Many polyfluorene derivatives have been prepared and investigated to afford materials with improved device efficiency and color purity for addressing the performance requirements for the next generation of plastic electronics and consumer demands.[5–7] Desired property improvements are possible by connecting the fluorene segments with vinylene linkages.[7–9] Their preparation uses Gilch and Horner–Emmons protocols, requiring rigorous reaction conditions such as anhydrous solvents and inert atmospheres. These coupling methods, unfortunately, produce significant byproducts requiring product purification in order not to compromise the material's colour emission and device performance.

Azomethines (–N=C–) are highly attractive alternatives to vinylene linkages owing to their easy preparation not requiring stringent reaction conditions.[10] They are further advantageous because their preparation is environmentally friendly with water being the unique byproduct produced. The preparation of azomethines, therefore, requires little or no purification. Moreover, the azomethine bond is isoelectronic to its all-carbon counterpart, making it ideally suited for func-

Received 5 May 2010. Accepted 6 June 2010. Published on the NRC Research Press Web site at canjchem.nrc.ca on 18 August 2010.

S. Barik, S. Friedland,[1] and W. Skene.[2] Centre of Self-Assembled Chemical Structures, Département de Chimie, Université de Montréal, CP 6128, succ. Centre-ville, Montréal, QC H3C 3J7, Canada.

[1]Present address: Department of Chemistry, McGill University, Montreal, QC, Canada.
[2]Corresponding author (e-mail: w.skene@umontreal.ca).

Chart 1. Monomers and oligomers prepared and investigated and some representative analogues.

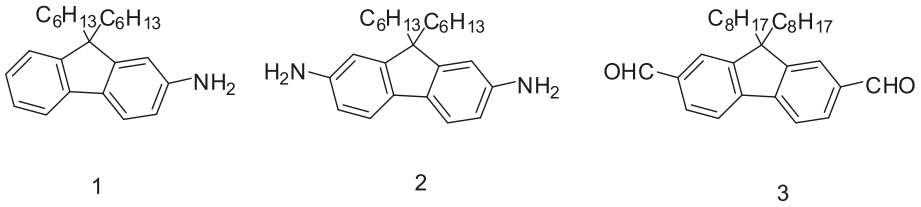

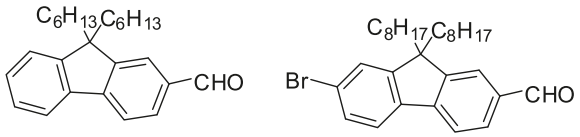

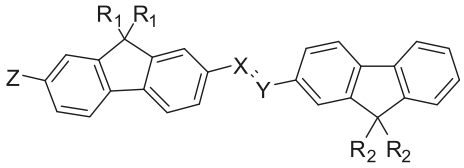

6 X = CH; Y = N; Z = CHO; $R_1 = C_8H_{17}$; $R_2 = C_6H_{13}$
7 X = N; Y = CH; $R_1 = R_2 = Z = H$

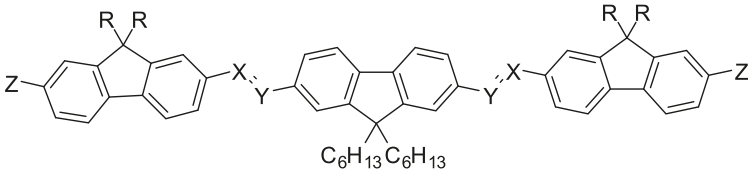

8 X = CH; Y = N; R = Z = H
9 X = CH; Y = N; Z = Br, $R = C_8H_{17}$

tional materials usage, but with the advantage of simple preparation and little purification.[11–13]

Despite these advantages, azomethine fluorenes have not been fully exploited as functional materials in emitting devices. This is a result of previously investigated fluorenylazomethine derivatives that were irreversibly oxidized and were nonfluorescent.[14,15] Such properties, unfortunately, preclude their use in functioning devices, and as a result, have attracted little attention for property improvement. It is therefore important to understand the reasons for irreversible oxidation to design and prepare new azomethine derivatives with functional materials properties. For this reason, we investigated the effect of fluorenylazomethine structure on the electrochemical properties to achieve reversible oxidation. We were further enticed to undertake such structure–property studies to bring to light the potential uses of fluorenylazomethines as functional materials. This is in part because azomethines are dismissed as useful functional materials owing to the limited properties of previously examined compounds. We therefore examined the electrochemical properties of a series of model fluorenylazomethines complemented with theoretical studies to better understand the oxidation process. The knowledge gained from such studies is not only pivotal for demonstrating the suitability of azomethines as functional materials, but also for designing and preparing future generations of fluorenyl compounds with tailored properties for specific applications. Herein, we present the preparation and electrochemical studies of a series of fluorenylazomethines, represented in Chart 1, for understanding the structure–reversible oxidation relationship.

Experimental

Materials and general experimental procedures

All reagents were commercially available from Sigma-Aldrich and were used as received unless otherwise stated. Anhydrous and deaerated solvents were obtained via a Glass Contour Solvent Purification System. ^{1}H NMR and ^{13}C NMR spectra were recorded on a Bruker 400 MHz spectrometer with the appropriate deuterated solvents.

Spectroscopic measurements

Absorption measurements were performed on a Cary-500 spectrometer and fluorescence studies were done on an Edinburgh Instruments FLS-920 fluorimeter after deaerating the samples thoroughly with nitrogen for 20 min. Relative fluorescence quantum yields were measured at 10^{-5} mol/L by exciting the corresponding compounds at its maximum absorption in spectroscopic grade dichloromethane relative to itself at 77 K under the same conditions.

Electrochemical measurements

Cyclic voltammetric measurements were performed on a Bio Analytical Systems EC Epsilon potentiostat at scan rates of 100 mV/s. Compounds were dissolved in anhydrous and deaerated dichloromethane at 10^{-4} mol/L with 0.5 mol/L Bu_4NPF_6. A platinum electrode and a saturated Ag/AgCl electrode were employed as auxiliary and reference electrodes, respectively, and ferrocene was added at the end of the electrochemical measurements to serve as an internal reference.

The highest occupied molecular orbital (HOMO) and lowest unoccupied molecular orbital (LUMO) energy levels and spin densities were calculated using density functional theory (DFT) calculation methods available in Spartan 06 (Wavefunction, Inc.) with the 6-31g* basis set.[16] The bond angles, distances, torsions, and other parameters were experimentally derived from the X-ray data for an analogous compound. The crystallographic data were used as the optimized geometry from which the single point energy was calculated to semiempirically calculate the molecular orbitals and spin densities. The rotational barriers were semiempirically calculated using the AM1 method.[17] The desired dihedral angel was varied from 0° to 360° and constrained at a given angle. The heat of formation (ΔH_f) for the given angle was subsequently calculated without additional structural optimization.

Synthetic procedures

The syntheses of **3**, **4, 7**, and **8** were prepared according to reported procedures.[18]

9,9-Dihexylfluorene

Fluorene (5 g, 30.8 mmol) was dissolved in DMSO (50 mL) and triethylbenzyl ammonium bromide (0.1 g, 1.5 mol) was added under N_2.[19] A 50% aqueous NaOH (15 mL) solution was added while stirring at room temperature. After 0.5 h, 1-bromohexane (12.41 g, 75.2 mmol) was added dropwise for 15 min. The reaction mixture was then stirred at room temperature for 4 d. The reaction mixture was diluted with an excess of diethyl ether and the aqueous layer was removed. The organic layer was washed with water, 2 mol/L HCl, and brine and then dried over $MgSO_4$. The solvent was removed under vacuum and the residue was purified by column chromatography over silica gel with hexanes as eluent to give the product as a white solid at –40 °C (7.8 g, 90%). ^{1}H NMR (400 MHz, $CDCl_3$) δ: 7.73 (d, 2H), 7.31–7.38 (m, 6H), 1.99 (dd, 4H), 1.07–1.33(m, 12H), 0.77 (t, 4H), 0.63(t, 6H). ^{13}C NMR (100 MHz, $CDCl_3$) δ: 151.1, 141.5, 127.4, 121.1, 123.2, 120.0, 55.4, 40.8, 31.9, 30.1, 24.1, 23.0, 14.2.

2,7-Dinitro-9,9-dihexylfluorene

The nitration was done similarly to published procedures.[20] A solution of 9,9-dihexylfluorene (2.12 g, 6.33 mmol) in 20 mL of HNO_3 in a 100 mL roundbottom flask was heated to reflux for 2 h under N_2 atmosphere. The reaction mixture was then cooled to room temperature and poured onto ice and the product was extracted with dichloromethane. The organic layer was washed with water three times, saturated $NaHCO_3$, and brine solution and then finally dried over $MgSO_4$. The solvent was evaporated and the crude product was purified by column chromatography with hexanes/ethyl acetate (7:3) to give a mixture of 2-nitro-9,9-dihexylfluorene and 2,7-dinitro-9,9-dihexylfluorene. The products were further recrystalized from EtOH to separate the two products, which were isolated as yellow solids.

2,7-Dinitro-9,9-dihexylfluorene

Isolated yield of 66% (1.94 g). ^{1}H NMR (400 MHz, $CDCl_3$) δ: 8.33 (dd, 2H), 8.28 (d, 2H), 7.93 (d, 2H), 2.09 (dd, 4H), 1.02–1.13 (m, 12H), 0.76 (t, 4H), 0.55 (t, 6H). ^{13}C NMR (100 MHz, $CDCl_3$) δ: 152.7, 147.5, 127.7, 123.6, 121.6, 120.1, 56.0, 40.4, 31.8, 29.9, 24.1, 22.9, 14.3.

2-Nitro-9,9-dihexylfluorene

^{1}H NMR (400 MHz, $CDCl_3$) δ: 8.27 (d, 1H), 8.23 (d, 1H), 7.82 (dd, 2H), 7.41–7.44 (m, 3H), 2.03 (dd, 4H), 1.05–1.13 (m, 12H), 0.76 (t, 4H), 0.60 (t, 6H). ^{13}C NMR (100 MHz, $CDCl_3$) δ: 152.7, 152.3, 148.0, 147.5, 129.6, 127.8, 123.6, 123.5, 121.6, 120.1, 118.6, 56.0, 40.5, 31.8, 29.9, 24.1, 22.9, 14.3.

2-Amino-9,9-dihexylfluorene (1)

2-Nitro-9,9-dihexylfluorene (0.84 g, 2.21 mmol) was dissolved in 10 mL of EtOH and stirred at room temperature under N_2. A catalytic amount of 10% Pd/C (0.2 g) was added followed by the addition of hydrazine monohydrate (1.6 g, 11.05 mmol) and the mixture was refluxed for 2 h. The reaction mixture was filtered to remove the Pd/C and the product was extracted with dichloromethane. The organic layer was washed with water (3 × 50 mL) and brine solution and then dried over $MgSO_4$. The solvent was evaporated and the crude product was purified by column chromatography with hexanes/ethyl acetate (1:1) as eluent to give the product as a brown sticky liquid with an isolated yield of 78%. The product was unstable and was kept under N_2 atmosphere and used immediately for subsequent reactions. ^{1}H NMR (400 MHz, $CDCl_3$) δ: 7.57 (d, 1H), 7.48 (d, 1H), 7.26 (m, 3H), 7.19 (dd, 2H), 6.68 (d, 2H), 1.90 (dd, 4H), 1.04 (m, 12H), 0.78 (t, 6H), 0.64 (d, 4H). ^{13}C NMR (100 MHz, $CDCl_3$) δ: 153.0, 150.1, 148.2, 128.9, 125.7, 122.9, 120.9, 118.7, 114.3, 110.2, 55.1, 41.0, 31.9, 30.2, 24.1, 23.0, 14.4. MS *m/z*: 350.54 (M^+).

2,7-Diamino-9,9-dihexylfluorene (2)

The solution of 2,7-dinitro-9,9-dihexylfluorene (1.2 g, 2.8 mmol) in 20 mL of EtOH was stirred at room temperature under N_2. To the above solution, a catalytic amount of 10% Pd/C (0.1 g) was added followed by hydrazine monohydrate (1.02 g, 20.18 mmol) and the mixture was refluxed for 2 h. The reaction mixture was filtered and the product was extracted with dichloromethane. The organic layer was washed with water (3 × 50 mL) and brine solution and then dried over $MgSO_4$. The solvent was evaporated and the crude product was purified by column chromatography with hexanes/ethyl acetate (1:1) to afford the title compound as a brown liquid with an isolated yield of 72%. The product was unstable and was stored under N_2 until used. ^{1}H NMR (400 MHz, $CDCl_3$) δ: 7.35 (d, 2H), 6.66 (d, 4H), 3.94 (br, NH_2), 1.83 (dd, 4H), 1.06 (m, 12H), 0.78 (t, 6H), 0.66 (d, 4H). ^{13}C NMR (100 MHz, $CDCl_3$) δ: 152.1, 144.3, 133.8, 119.5, 114.6, 110.7, 55.0, 41.3, 32.0, 30.2, 24.1, 23.1, 14.4. MS *m/z*: 356.3 (M^+).

9,9-Dioctylfluorene-2,7-dicarboxaldehyde (3)

A 250 mL two-necked flask containing 9,9-dioctyl-2,7-dibromofluorene (2.2 g, 4.01 mmol) in anhydrous THF (40 mL) was stirred under N_2 at –78 °C in an acetone–dry ice bath.[21] *n*-Butyl lithium (7.6 mL, 16.0 mmol) was added under vigorous stirring and stirred for 1.5 h. A deaerated mixture of DMF (5 mL) and anhydrous THF (3 mL) was added dropwise to the reaction mixture at –78 °C and allowed to stir for 1 h at room temperature. The reaction mixture was cooled to 0 °C and 10% HCl was added until the solution was acidic (tested by litmus paper). After stirring for 30 min, the mixture was partitioned between dichloromethane and water and the organic layer was isolated. The aqueous layer was washed with dichloromethane and the combined organic extracts were dried over Na_2SO_4. The crude product was purified by column chromatography using hexanes/dichloromethane (1:1) as eluent. The product was obtained as colourless crystals (58%, 1.05 g). ^{1}H NMR (400 MHz, $CDCl_3$) δ: 10.1 (s, 2H, CHO), 7.91–7.96 (m, 6H), 2.0 (dd, 4H), 1.02 (m, 20H), 0.78 (t, 6H), 0.56 (d, 4H). ^{13}C NMR (100 MHz, $CDCl_3$) δ: 192.5, 153.2, 146.0, 136.8, 130.7, 123.8, 121.7, 56.0, 40.4, 32.1, 30.2, 29.5, 24.2, 22.9, 14.4. MS *m*/*z*: 446.4 (M^+).

9,9-Dihexylfluorene-2-carboxaldehyde (4)

The synthesis was followed according to known methods.[17] The solution of 2-bromo-9,9-dihexylfluorene (4.0 g, 9.67 mmol) in anhydrous THF (50 mL) was purged with N_2 at –78 °C in an acetone–dry ice bath. To the above solution, *n*-butyl lithium (9.21 mL, 19.35 mmol) was added dropwise and stirred for 1.5 h. A degassed solution of DMF (2 mL) and anhydrous THF (3 mL) was added dropwise while maintaining the reaction mixture at –78 °C, after which the temperature was raised to room temperature and stirred for 1 h. The reaction mixture was cooled to 0 °C and 10% HCl was added until the solution was acidic as verified by litmus paper. After stirring for 30 min, the mixture was partitioned between dichloromethane and water. The organic layer was extracted and the aqueous layer was washed again with dichloromethane. The combined organic fractions were dried over Na_2SO_4. After solvent removal, the crude product was purified by column chromatography with hexanes/dichloromethane (1:1). The product was obtained as a colourless liquid (2.15 g, 48%). ^{1}H NMR (400 MHz, $CDCl_3$) δ: 10.09 (s, 1H, CHO), 7.91 (s, 1H), 7.86 (dd, 2H), 7.97 (dd, 1H), 7.41 (m, 3H), 2.02 (dd, 4H), 1.04 (m, 12H), 0.75 (t, 6H), 0.569 (d, 4H). ^{13}C NMR (100 MHz, $CDCl_3$) δ: 192.7, 152.5, 147.9, 139.9, 135.7, 130.9, 129.2, 127.5, 123.5, 123.4, 121.3, 120.3, 55.8, 40.64, 31.8, 30.0, 29.5, 24.1, 22.9, 14.4. MS *m*/*z*: 363.24 (M^+).

2-Bromo-9,9-dioctylfluorene-7-carboxaldehyde (5)

To the solution containing 9,9-dioctyl-2,7-dibromofluorene (3.0 g, 5.47 mmol) in anhydrous THF (60 mL) purged with N_2 at –78 °C was added *n*-butyl lithium (2.84 mL, 7.11 mmol) and the reaction was allowed to stir for another 1.5 h. Afterwards, deaerated DMF (1 mL) diluted in anhydrous THF (1 mL) was added dropwise to the reaction mixture at –78 °C, after which the temperature was allowed to warm to room temperature and then stirred for 1 h. The reaction mixture was cooled to 0 °C and 10% HCl was added until the solution was acidic. The solution was stirred for 30 min then the product was extracted in dichloromethane. The organic layer was isolated while the aqueous layer was washed with dichloromethane once more and the combined organic extracts were dried over Na_2SO_4. The crude product was purified by column chromatography with hexanes/dichloromethane (1:1) to afford the title product as colorless crystals (0.9 g, 58%). ^{1}H NMR (400 MHz, $CDCl_3$) δ: 10.08 (s, 1H, CHO), 7.83–7.88 (m, 3H), 7.64 (d, 1H), 7.51 (d, 2H), 2.01 (dd, 4H), 1.05 (m, 20H), 0.81 (t, 6H), 0.57 (d, 4H). ^{13}C NMR (100 MHz, $CDCl_3$) δ: 192.5, 154.6, 151.5, 146.7, 138.9, 136.0, 130.9, 130.8, 126.8, 123.5, 122.6, 120.5, 56.0, 40.4, 32.1, 32.0, 30.2, 29.5, 24.1, 22.9, 14.4, MS *m*/*z*: 497.0 (M^+).

7-[(9′,9′-Dihexylfluoren-2′-ylimino)-methyl]-9,9-dioctylfluorene-2-carboxaldehyde (6)

Both **3** (100 mg, 0.22 mmol) and **1** (180.1 mg, 0.514 mmol) were dissolved in absolute ethanol under N_2. A catalytic amount of TFA (60 μL of 1% in absolute ethanol) was added and the reaction mixture was stirred overnight at room temperature. The solvent was evaporated to afford a dark oil that was extracted with dichloromethane (25 mL). The organic layer was washed with water and brine solution and then dried over $MgSO_4$. The crude product was chromatographed on activated basic alumina with ethyl acetate/hexanes (1:1 *v*/*v*) to yield the product as a yellow oil (80 mg, 60%). ^{1}H NMR (400 MHz, $CDCl_3$) δ: 10.08 (s, 1H), 8.65 (s, 1H), 8.00 (s, 1H), 7.89 (m, 4H), 7.86 (m, 3H), 7.74 (d, 1H, J = 7.3 Hz), 7.41 (s, 1H), 7.4 (t, 1H, J = 7.3 Hz), 7.31 (m, 2H), 2.01 (m, 8H), 1.08 (m, 30 H), 0.79 (t, 12H, J = 7.0 Hz), 0.61 (m, 8H). ^{13}C NMR (100 MHz, $CDCl_3$) δ: 192.8, 160.7, 152.5, 152.4, 151.9, 151.2, 147.9, 139.9, 135.7, 130.9, 129.2, 127.5, 127.3, 127.1, 123.5, 123.4, 121.3, 120.3, 119.8, 116.5, 55.6, 40.6, 32.0, 31.9, 31.8, 30.1, 30.0, 24.2, 24.1, 23.1, 23.0, 22.9, 14.4, 14.3. MS *m*/*z*: 778.49.

2′,7′-[(9,9,9″,9″-Tetraoctylfluorene-7,7″-diylimino)-methyl]-9′,9′-dihexyl-2,2″-dibromotrifluorene (9)

Both **6** (0.511 g, 1.02 mmol) and **4** (0.150 g, 0.411 mmol) were dissolved in absolute ethanol (5 mL) under N_2. TFA (60 μL of 1% in ethanol) was added to the reaction mixture and then it was stirred for 1 h at room temperature. The solvent was evaporated to afford a brown oil that was extracted with dichloromethane (25 mL). The organic layer was washed with water (2 × 50 mL) and brine solution (2 × 50 mL) and then dried over $MgSO_4$. The product was isolated as a yellow solid (44%) after flash column chromatography with basic activated alumina with hexanes/ethyl acetate (7:3). ^{1}H NMR (400 MHz, $CDCl_3$) δ: 8.64 (d, 2H), 7.9 (d, 4H), 7.62 (dd, 4H), 7.52 (d, 4H), 7.31 (d, 2H), 6.65 (4H), 2.06 (dd, 12H), 1.08 (m, 50H), 0.81 (m, 18H), 0.63 (m, 12H). ^{13}C NMR (100 MHz, $CDCl_3$) δ: 160.3, 154.1, 153.2, 152.6, 151.4, 146.2, 143.8, 140.5, 139.8, 139.7, 136.2, 136.0, 132.5, 130.5, 129.3, 126.7, 122.8, 122.0, 120.7, 120.3, 119.6, 119.2, 116.4, 114.4, 110.2, 56.0, 55.3, 41.2, 40.6, 32.0, 30.4, 30.3, 30.2, 29.6, 24.1, 24.0, 23.0, 22.9, 14.4. MS *m*/*z*: 1323.6 (M^+).

Results and discussion

Synthesis

Compounds **6–9** were prepared and investigated to provide insight into the fluorescence and electrochemical behaviour of fluorenylazomethines. The compounds were chosen as model compounds for such studies given the complexity of absolute characterization of their polymeric counterparts. The advantage of investigating these model compounds is that precise structure–property relationships can be accurately obtained. The compounds were judiciously selected because the effect of the imine bond, 9-fluorenyl alkylation, degree of conjugation, and substitution of the fluorene's 2,7-positions on both the electrochemical and photophysical properties could be investigated. The required fluorenyl aldehyde precursors were prepared from 9,9-dioctyl 2,7-dibromofluorene by standard metal–halogen exchange with *n*-butyl lithium and quenching with DMF.[22] The various aldehyde derivatives were obtained by varying the *n*-BuLi/dibromofluorene ratio. The complementary aminofluorene derivatives were obtained by nitrating 9,9-dihexyl-fluorene, prepared from fluorene by known methods, followed by reduction with activated Pd/C (10%).[23] The resulting amino fluorenes were extremely sensitive to ambient conditions and underwent spontaneous decomposition. Consequently, they were used immediately once synthesized for preparing the targeted azomethines. The desired azomethines were prepared using mild coupling conditions by refluxing the complementary fluorenes in absolute ethanol in the presence of a catalytic amount of TFA. The desired products were readily purified by column chromatography without any decomposition and were obtained in sufficient purity for electrochemical and spectroscopic characterization. The extended degree of conjugation of **6–9** make these compounds stable and less sensitive to acid hydrolysis to their aliphatic counter parts.

Electrochemical studies

The electrochemical behaviour is an important property for functional materials. Given that the exciton in an emitting device is produced by the recombination of an electron and hole, it is desired that the emitting layer be able to repeatedly sustain the harsh oxidation and reduction environment found in the device environment for ensuring device longevity. The redox properties of the fluorenylazomethines were therefore investigated and the structure-redox potentials examined. The effects of substitution in the 2, 2′-positions, degree of conjugation, and alkylation on the electrochemical properties are possible with the compounds in Chart 1.

The effect of the single heteroatomic bond on the E_{pa} is evident by comparing **6** with **4**. The oxidation potential of the fluorenylazomethine is increased by 130 mV. Although the E_{pa} of **6** is expected to be reduced significantly compared to **4** as a result of the increased degree conjugation arising from the azomethine bond, the heteroconjugated bond is a good electron-withdrawing group and counterbalances some of the energetic gain from the increased conjugation. The E_{pa} of **7** is increased relative to **6** owing to the absence of the electron-withdrawing aldehyde group. Meanwhile, the E_{pa} of **8** is 120 mV lower than **7** because of its

Fig. 1. Cyclic voltammogram of **6** (●) and **9** (○) measured at 100 mV/s.

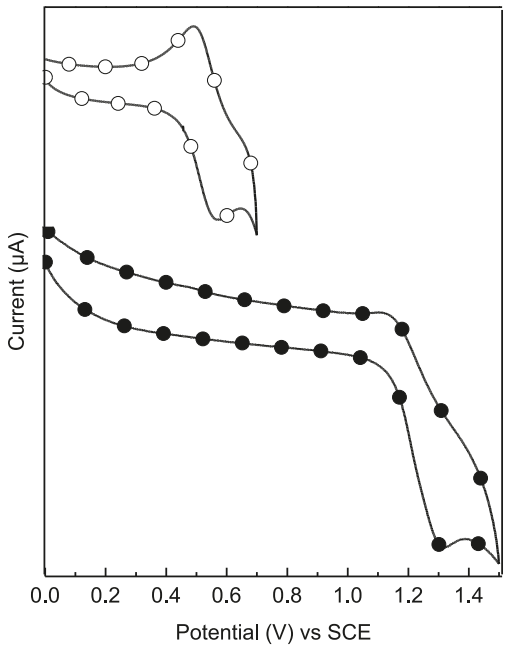

increased degree of conjugation. A significantly larger decrease in the oxidation is expected for **8** as a result of the increased degree of conjugation; however, previous crystallographic studies showed that the terminal fluorenes are highly twisted with respect to the central axis.[24] Therefore, it has a limited degree of conjugation, located predominantly on the =N–fluorene–N= central moiety. Conversely, **9** is highly conjugated according to the extremely low E_{pa} measured. The difference in conjugation between **8** and **9** is most likely a result of the alkyl substitution that forces coplanarization of the fluorene and azomethine units to minimize interchain interactions. Although unequivocal confirmation of the extended conjugation can be had from the crystal structure, repeated attempts to crystallize **9** were, unfortunately, unsuccessful. The optimized geometry was subsequently calculated via DFT for examining the structure of **9**. We first tested this method for accurately calculating the optimized azomethine geometries by comparing calculated structures with those measured experimentally from known crystal structure data. The calculated optimized geometries were consistent with those obtained by X-ray diffraction (XRD). The resulting structure calculated for **9** showed the terminal fluorenes to be twisted by 12° from the plane described by the central fluorene and the azomethines. This is in contrast to **8**, whose terminal fluorenes are twisted by 26.7° and 65.3° from the central fluorene plane.[18,25] The low E_{pa} of **9** relative to the other azomethines is therefore a result of both its extended degree of conjugation and the weak electron-donating terminal bromines.

As seen in Fig. 1, the first oxidation process of **9** is reversible. This is in contrast to the other fluorenylazomethines, such as **6**, that undergo irreversible oxidation. The electrochemical sample of **9** was thoroughly deaerated to ensure that the observed reversible process was not from the reduction of residual oxygen. The peak persisted despite persistent nitrogen purging. The anodic process corresponds to a one-

Fig. 2. Calculated spin densities shown in red for the radical cation **9**. The alkyl groups in the 9-positions are omitted for clarity.

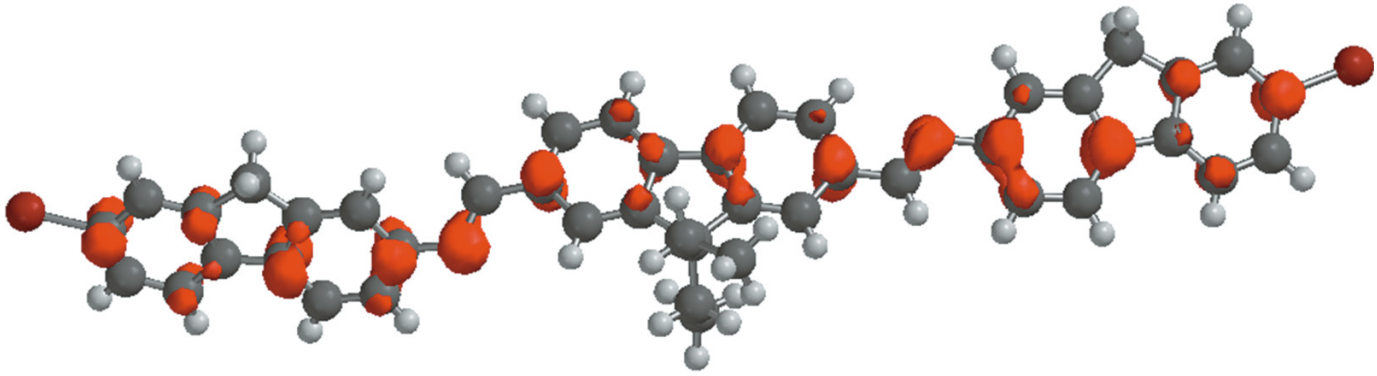

Fig. 3. Normalized fluorescence spectra of **2** (▲), **3** (◆), **6** (★), and **9** (●) excited at their respective maximum. Inset: normalized emission spectra of **9** at room temperature (△) and 77 K (▲).

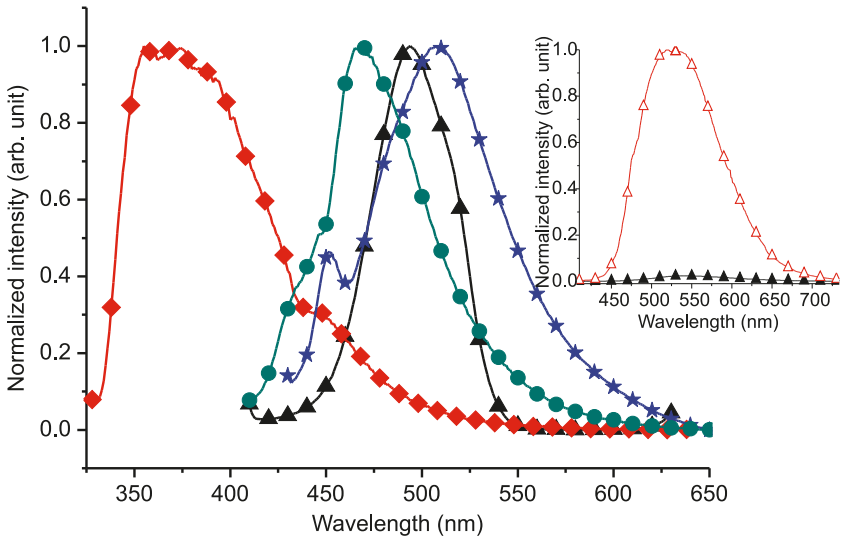

electron transfer process while oxygen reduction is a two-electron process. The radical cation produced from the one-electron oxidation of **9** is therefore stable, based on the observed reversible oxidation, while similar intermediates for the other azomethines are unstable, evidenced by the irreversible anodic processes.

The spin densities of the radical cation of **9** were investigated to understand the reversible anodic behaviour. As seen in Fig. 2, the calculated spin densities is evenly distributed over most of the carbons of **9**. The 2,2′-positions are substituted with bromine for **9** while for the other azomethines, such as **6**–**8**, these positions are unsubstituted. Therefore, the resulting radical cation undergoes homocross-coupling according to known means when it is located in the terminal position.[26] This leads to the irreversible oxidation, as observed for **6**–**8**.[27,28] The terminal halogens of **9** effectively prevent radical cross-coupling and make the one-electron transfer process reversible. Alkylation in the 9-position is also important for reversible radical cation formation, according to Fig. 2. Azomethine structure and substitution play important roles in determining both the oxidation potentials at which the radical cation is produced and its reversible formation. The fluorenylazomethine oxidation potentials and the reversibility of these processes can thus be tuned courtesy of substitution in the 2,2′-positions. It is therefore expected that polymers derived from **2** and **3** should sustain reversible oxidation.

Fluorescence studies

Fluorescence investigations involving previously studied azomethines have exclusively used relative actinometry. The challenge with this approach is the lack of universal reference whose emission yield is accurately known and is both wavelength and solvent independent. Also, there is no general actinometer that consistently absorbs across the entire visible spectrum for measuring the emission yields of highly conjugated compounds regardless of the degree of conjugation. As a result of these limitations, large variations of fluorescence quantum yields are reported and cannot be accurately known. The absolute quantum yields of the fluorenylazomethine model compounds and their precursors were therefore measured using an integrating sphere because of their variable absorbance and fluorescence, evident in Fig. 3. As seen in Table 1, the fluorescence yields of the precursors **1**–**5** are all quenched. This is not surprising given that the fluorescence of fluorene is highly dependent on substitution.[29,30] The addition of the azomethine bond to the flu-

Table 1. Photophysical and electrochemical properties of fluorenylazomethine derivatives and their precursors.

Compound	λ_{abs} (nm)	λ_{em} (nm)	Φ_{fl} (77 K)[a]	E_g (eV)[b]	E_{pa} (V)[c]	E_{pc} (V)[d]	HOMO (eV)[e]	LUMO (eV)[e]	E_g (eV)[f]
Fluorene[g]	261	302	0.72	3.9	1.36	–1.31	5.2	3.3	1.9
1[h]	292	389	0	3.5	—	—	—	—	—
2[h]	398	494	0.01	2.5	—	—	—	—	—
3	339	383	0	3.4	1.00	–1.02	5.4	3.4	2.0
4	326	366	0.01	3.5	1.15	–1.06	5.8	3.3	2.5
5	330	425	0.02	3.4	0.86	–1.90	5.26	2.5	2.76
6	384	509	0.02 (0.32)	2.6	1.30	–1.64	5.7	2.8	2.9
7[i]	361	445	0.01 (0.05)	2.9	1.53	–1.12	5.6	3.5	2.1
8[i]	396	472	0.01 (0.31)	2.8	1.41	–1.52	5.6	3.4	2.2
9	410	470	0.02 (0.38)	2.6	0.56	—	4.9	2.3	2.6

[a]Fluorescence quantum yield at room temperature. Values in parentheses are the emission yields measured at 77 K and calculated relative to the absolute room temperature fluorescence yields.

[b]Spectroscopically determined energy gap taken from the absorption onset.

[c]Oxidation potential relative to saturated Ag/Ag^+ electrode.

[d]Reduction potential relative to Ag/Ag^+.

[e]Relative to the vacuum level.

[f]Electrochemical energy gap.

[g]Reference 25.

[h]Reliable electrochemical data for **1** and **2** could not be obtained as a result of their instability under our experimental conditions.

[i]Reference 18.

orene moiety does not increase the fluorescence. In all cases, the fluorenylazomethine fluorescence is quenched regardless of degree of oligomerization.

With increasing oligomerization, the number of degrees of freedom increases, representing additional modes of fluorescence deactivation. Fluorescence deactivation by aryl–azomethine bond rotation was subsequently investigated to determine whether this deactivation mode was responsible for the quenched azomethine fluorescence. This was done by examining the fluorescence emission at 77 K, at which temperature all nonradiative fluorescence deactivation modes by bond rotation are suppressed. Therefore, fluorescence increase is expected at 77 K if deactivation by nonradiative means occurs. The oligofluorenes **6**–**9** all exhibited significant increases in fluorescence yields at this reduced temperature as seen in the inset of Fig. 3. Unfortunately, accurate quantitative measurements of the emission yields at 77 K cannot be obtained because they are reliant on the weak room temperature fluorescence signals. Nonetheless, the fluorescence quantum yields of the oligofluorenylazomethines at low 77 K surpass those of their precursors at room temperature and reach the same order of magnitude as native fluorene.

To provide further insight into the origins of the temperature dependent fluorescence of the azomethines, the rotational barrier around the =N–fluorenyl and =CH–fluorenyl bonds were semiempirically calculated. A simple alkylated dyad analogue of **7** was used as a model compound because its crystal structure data is known, which were used for inputting the correct optimized ground state geometry. The heats of formation (ΔH_f) of each torsion around the fluorene–N= and =CH–fluorene bonds were calculated. Although absolute ΔH_f values are not possible as a result of scaling errors, the relative values can, however, be accurately calculated. The semiempirically calculated bond rotation energies for an analogous fluorene–fluorene dyad were also calculated. 2,2′-Bifluorene was used as a benchmark

Fig. 4. Rotational bond energies of the fluorene–N= (black) and =CH–fluorene (blue) bonds for **6** and 2,2′-bifluorene (red) semiempirically calculated from the heats of formation (ΔH_f) using AM1.

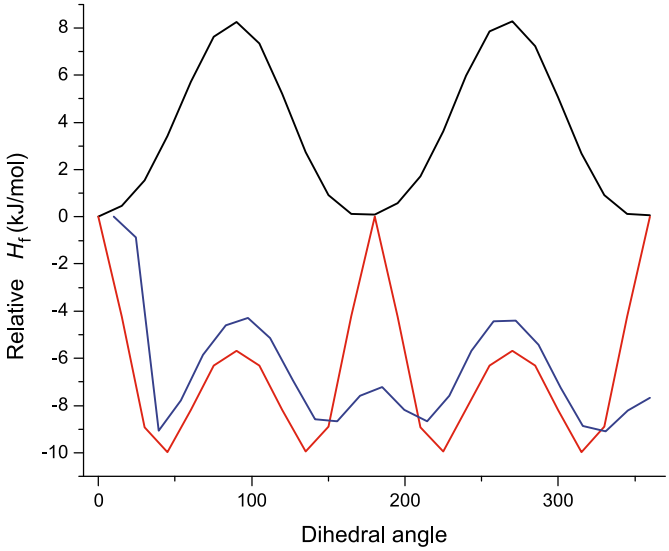

since its fluorescence yields are reduced relative to native fluorene as a result of nonradiative deactivation around the fluorene–fluorene bond.[24] As seen in Fig. 4, the bond rotation energies for both the azomethine and fluorene dyads are similar. This suggests that fluorescence quenching by nonradiative bond rotation is a possible deactivation mode for azomethines. The absolute fluorescence yield of **9** was subsequently examined in thin films, where bond rotation deactivation processes cannot occur. A fluorescence quantum yield of 0.08 was measured in the solid state, confirming that deactivation by means other than simple fluorene–N= and =CH–fluorene bond rotation as responsible for azomethine fluorescence quenching. Meanwhile, the fluores-

cence of both **6** and **9** could, however, be significantly restored by protonating the azomethine bond with TFA. The measured absolute fluorescence yield for these two compounds was 0.4 and 0.11, respectively. The fluorescence on/off switching by acid protonation corroborates previous studies that the major deactivation mode is by intramolecular photoinduced electron transfer.[31] Fluorenylazomethines are therefore interesting because their fluorescence can be tuned by both temperature and acid doping.

Conclusion

A series of dyad and triad fluorenylazomethines were prepared with different electronic groups and substitution. The oxidation potential was contingent on both substitution and degree of conjugation. Although homoaryl groups are normally twisted by up to 65° from the azomethines to which they are linked, increased planarity and hence increased degree of conjugation was possible by alkylating the fluorene's 9-position. Substitution in the 2,2′-position was also found to play an important role in determining the reversibility of the electrochemically generated radical cation. Meanwhile, the fluorescence of the azomethines remained quenched similar to their precursors. The fluorescence could be restored at low temperature and by acid protonation. The fluorenylazomethines therefore have sensor properties. The collective knowledge gained from the combined electrochemical and fluorimetric studies is pivotal for the design and preparation for the future generation of azomethines for emitting applications and will lead to highly fluorescent materials with desired reversible oxidation. The results further suggest that polymers derived from **2** and **3** will exhibit desired reversible oxidation, making them suitable materials for emitting applications.

Supplementary data

Supplementary data for this article are available on the journal Web site (canjchem.nrc.ca).

Acknowledgements

The Natural Sciences and Engineering Reserach Council of Canada (NSERC) is thanked for a Discovery Grant (DG) and a Research Tools and Instruments (RTI) Grant, and the Centre for Self-Assembled Chemical Structures (CSACS) for a Strategic Research Grant (SRG), which allowed this work to be performed. In addition, the Canada Foundation for Innovation (CFI) is thanked for additional equipment funding. WGS also thanks both the Alexander von Humboldt Foundation and the Royal Society of Chemistry (RSC) for a J. W. T. Jones Travelling Fellowship, allowing this manuscript to be completed. SF thanks NSERC and the Reactive Intermediate Student Exchange Program (RISE) program for an undergraduate scholarship.

References

(1) Brédas, J.-L.; Norton, J. E.; Cornil, J.; Coropceanu, V. *Acc. Chem. Res.* **2009**, *42* (11), 1691. doi:10.1021/ar900099h. PMID:19653630.

(2) Bredas, J.-L.; Durrant, J. R. *Acc. Chem. Res.* **2009**, *42* (11), 1689. doi:10.1021/ar900238j. PMID:19916562.

(3) Kamtekar, K. T.; Monkman, A. P.; Bryce, M. R. *Adv. Mater.* **2010**, *22* (5), 572. doi:10.1002/adma.200902148. PMID: 20217752.

(4) Lee, K.; Nair, P. R.; Scott, A.; Alam, M. A.; Janes, D. B. *J. Appl. Phys.* **2009**, *105* (10), 102046. doi:10.1063/1.3116630.

(5) Simas, E. R.; Gehlen, M. H.; Glogauer, A.; Akcelrud, L. *J. Phys. Chem. A* **2008**, *112* (23), 5054. doi:10.1021/jp711934d. PMID:18481838.

(6) Zhang, K.; Chen, Z.; Yang, C.; Zou, Y.; Gong, S.; Qin, J.; Cao, Y. *J. Phys. Chem. C* **2008**, *112* (10), 3907. doi:10.1021/jp077433+.

(7) Mikroyannidis, J. A.; Gibbons, K. M.; Kulkarni, A. P.; Jenekhe, S. A. *Macromolecules* **2008**, *41* (3), 663. doi:10.1021/ma071504l.

(8) Sun, M.; Zhong, C.; Li, F.; Cao, Y.; Pei, Q. *Macromolecules* **2010**, *43* (4), 1714. doi:10.1021/ma9024762. PMID:17343421.

(9) Bezgin, B.; Yagan, A.; Onal, A. M. *J. Electroanal. Chem.* **2009**, *632* (1–2), 143. doi:10.1016/j.jelechem.2009.04.011.

(10) Guarìn, S. A.; Bourgeaux, M.; Dufresne, S.; Skene, W. G. *J. Org. Chem.* **2007**, *72* (7), 2631. doi:10.1021/jo070100o. PMID:17343421.

(11) Wang, C.; Shieh, S.; LeGoff, E.; Kanatzidis, M. G. *Macromolecules* **1996**, *29* (9), 3147. doi:10.1021/ma9514131.

(12) Yang, C.-J.; Jenekhe, S. A. *Chem. Mater.* **1991**, *3* (5), 878. doi:10.1021/cm00017a025.

(13) Kuder, J. E.; Gibson, H. W.; Wychick, D. *J. Org. Chem.* **1975**, *40* (7), 875. doi:10.1021/jo00895a013.

(14) Tsai, F.-C.; Chang, C.-C.; Liu, C.-L.; Chen, W.-C.; Jenekhe, S. A. *Macromolecules* **2005**, *38* (5), 1958. doi:10.1021/ma048112o.

(15) Liu, C.-L.; Chen, W.-C. *Macromol. Chem. Phys.* **2005**, *206* (21), 2212. doi:10.1002/macp.200500236.

(16) Sherrill, C. D. *J. Chem. Phys.* **2010**, *132* (11), 110902. doi:10.1063/1.3369628.

(17) Thiel, W. In *Theory and Applications of Computational Chemistry: The First Forty Years;* Dykstra, C. E., Kim, K. S., Frenking, G., Scuseria, G. E., Eds.; Elsevier: Amserdam, 2005; pp 559–580.

(18) Guarìn, S. A. P.; Dufresne, S.; Tsang, D.; Sylla, A.; Skene, W. G. *J. Mater. Chem.* **2007**, *17* (27), 2801. doi:10.1039/b618098a.

(19) Chen, Q.-Q.; Liu, F.; Ma, Z.; Peng, B.; Wei, W.; Huang, W. *Chem. Lett.* **2008**, *37* (2), 178. doi:10.1246/cl.2008.178.

(20) Dudek, S. P.; Pouderoijen, M.; Abbel, R.; Schenning, A. P. H. J.; Meijer, E. W. *J. Am. Chem. Soc.* **2005**, *127* (33), 11763. doi:10.1021/ja052054k. PMID:16104754.

(21) Giuseppone, N.; Fuks, G.; Lehn, J.-M. *Chem. Eur. J.* **2006**, *12* (6), 1723. doi:10.1002/chem.200501037.

(22) Belfield, K. D.; Morales, A. R.; Kang, B.-S.; Hales, J. M.; Hagan, D. J.; Van Stryland, E. W.; Chapela, V. M.; Percino, J. *Chem. Mater.* **2004**, *16* (23), 4634. doi:10.1021/cm049872g.

(23) Dudek, S. P.; Pouderoijen, M.; Abbel, R.; Schenning, A. P. H. J.; Meijer, E. W. *J. Am. Chem. Soc.* **2005**, *127* (33), 11763. doi:10.1021/ja052054k. PMID:16104754.

(24) Guarin, S. A. P.; Dufresne, S.; Tsang, D.; Sylla, A.; Skene, W. G. *Polymeric Materials: Science and Engineering (PMSE) Preprints;* American Chemical Society: Washington, DC, 2007; Vol. 96, p 244.

(25) Dufresne, S.; Pérez Guarìn, S. A.; Bolduc, A.; Bourque, A. N.; Skene, W. G. *Photochem. Photobiol. Sci.* **2009**, *8* (6), 796. doi:10.1039/b819735k. PMID:19492107.

(26) Roncali, J. *Chem. Rev.* **1992**, *92* (4), 711. doi:10.1021/cr00012a009.

(27) Roncali, J.; Blanchard, P.; Frère, P. *J. Mater. Chem.* **2005**, *15* (16), 1589. doi:10.1039/b415481a.

(28) Hapiot, P.; Lagrost, C.; LeFloch, F.; Raoult, E.; Rault-Berthelot, J. *Chem. Mater.* **2005**, *17* (8), 2003. doi:10.1021/cm048331o.
(29) Turro, N. J.; Ramamurthy, V.; Scaiano, J. C. *Principles of Molecular Photochemistry: An Introduction;* University Science Books: Sausalito, CA, 2009.
(30) Murphy, R. S.; Moorlag, C. P.; Green, W. H.; Bohne, C. *J. Photochem. Photobiol. A* **1997**, *110* (2), 123. doi:10.1016/S1010-6030(97)00191-3.
(31) Dufresne, S.; Callaghan, L.; Skene, W. G. *J. Phys. Chem. B* **2009**, *113* (47), 15541. doi:10.1021/jp907391y.